Published in final edited form as:
Circ Arrhythm Electrophysiol. 2012 February ; 5(1): 32–42. doi:10.1161/CIRCEP.111.964197.

Functional Nature of Electrogram Fractionation Demonstrated by Left Atrial High Density Mapping

Amir S. Jadidi, MD[1], **Edward Duncan, PhD**[1], **Shinsuke Miyazaki, MD**[1], **Nicolas Lellouche, MD**[2], **Ashok J. Shah, MD**[1], **Andrei Forclaz, MD**[1], **Isabelle Nault, MD, FRCPC**[1], **Matthew Wright, MBBS, PhD**[1], **Lena Rivard, MD**[1], **Xingpeng Liu, MD**[1], **Daniel Scherr, MD**[1], **Stephen Wilton, MD**[1], **Frédéric Sacher, MD**[1], **Nicolas Derval, MD**[1], **Sebastien Knecht, MD**[1], **Steven J. Kim, MSEE**[3], **Mélèze Hocini, MD**[1], **Sanjiv Narayan, MD**[1], **Michel Haïssaguerre, MD**[1], and **Pierre Jaïs, MD**[1]

[1]Hôpital Cardiologique du Haut-Lévêque & Université Bordeaux II, Bordeaux, France

[2]Assistance Publique Hôpital Henri Mondor and INSERM U 841, Créteil, France

[3]St Jude Medical, St. Paul, MN

Abstract

Background—Complex fractionated electrograms (CFAE) are targets of atrial fibrillation (AF) ablation. Serial high density maps were evaluated to understand the impact of activation direction and rate on electrogram (EGM) fractionation.

Methods and Results—18 patients (9 persistent) underwent high density, 3D, left atrial mapping (>400 points/map) during AF, Sinus (SR) and CS-paced (CSp) rhythms. In SR and CSp, fractionation was defined as EGM with ≥4 deflections, while in AF CFEmean <80ms was considered as continuous CFAE. The anatomic distribution of CFAE sites was assessed, quantified and correlated between rhythms. Mechanisms underlying fractionation were investigated by analysis of voltage, activation and propagation maps. A minority of continuous CFAE sites displayed EGM fractionation in SR (15+/−4%) and CSp (12+/(12+/−8%). EGM fractionation did not match between SR and CSp at 70+/−10% sites. Activation maps in SR and CSp showed that wave collision (71%) and regional slow conduction (24%) caused EGM fractionation. EGM voltage during AF (0.59+/−0.58mV) was lower than during SR and CSp (>1.0mV) at all sites. During AF, the EGM voltage was higher at continuous CFAE sites than at non-CFAE sites (0.53mV (Q1, Q3: 0.33–0.83) vs. 0.30 mV (Q1, Q3: 0.18–0.515), p<0.00001). Global LA voltage in AF was lower in persistent vs. paroxysmal AF patients (0.6+/−0.59mV vs. 1.12+/−1.32mV, p<0.01).

Conclusions—The distribution of fractionated EGMs is highly variable, depending on direction and rate of activation (SR vs. CSp vs. AF). Fractionation in sinus and CSp rhythms mostly resulted from wave collision. All sites with continuous fractionation in AF displayed normal voltage in SR suggesting absence of structural scar. Thus, many fractionated EGMs are functional in nature and their sites dynamic.

Corresponding Author: Amir S. Jadidi, MD, Hôpital Cardiologique du Haut-Lévêque, Université Bordeaux II, 33604 Bordeaux-Pessac, France, Tel: + 33 668 19 91 43, Fax: + 33 5 57 65 68 96, amir.s.jadidi@gmail.com.

Conflict of Interest Disclosures: None.

Keywords

atrial fibrillation; CFAE; fractionation; wave collision; slow conduction; sinus rhythm; paced rhythm

Introduction

When combined with pulmonary vein isolation, ablation of fractionated electrograms (CFAE) is associated with higher acute and long-term success rates in patients with persistent atrial fibrillation (1;2). Different electrophysiological mechanisms may result in CFAE (3) and these complex EGMs can either actively contribute to AF perpetuation or alternatively be bystanders (4;5). Notably, the ablation of continuous CFAE sites is associated with a higher likelihood of AF cycle length prolongation and AF termination than ablation of intermittent CFAE activity (6). Indeed, CFAE ablation does not always impact upon AF cycle length confirming that not all are appropriate targets for ablation (7). Despite this, we currently largely ignore how to distinguish bystander from active CFAE in AF.

The aim of the current study is therefore to investigate the impact of different heart rhythms (AF, sinus rhythm (SR) and coronary sinus pacing (CSp)) upon left atrial CFAE properties in patients with atrial fibrillation, independent of any catheter ablation. Consistent LA fractionation during all rhythms may differentiate a local fixed atrial/anatomical substrate (structural remodelling) from wave collision or functional slow conduction. Moreover, acquisition of high density activation maps during SR and CSp allows analysis of the underlying mechanisms of fractionation.

Methods

21 patients with symptomatic, drug-refractory AF were enrolled. All anti-arrhythmic drugs except amiodarone were stopped at least 5 half-lives before the procedure. 6/9 patients with persistent AF and 5/9 in the paroxysmal AF group were on Amiodarone. All patients gave written informed consent for the study, which was approved by the institutional clinical research and ethics committee.

Electrophysiologic study

All patients received oral anticoagulation (target INR 2–3) for at least 1 month prior to the procedure and underwent transoesophageal echocardiography within 48 hours preceding the procedure to exclude the presence of thrombus. Electrophysiologic study was performed in the fasted state using conscious sedation.

The following catheters were introduced via the right femoral vein: (1) a deflectable decapolar catheter (Extreme, Sorin, France) was positioned within the coronary sinus (CS); (2) a 3.5mm externally irrigated-tip catheter (Thermocool, Biosense-Webster, CA) was used for ablation; (3) a 20-pole high-density double-loop mapping catheter AFocus II HD (St Jude Medical, Minneapolis, MN, USA) was used to create the left atrial geometry and also to map CFAE in the left atrium (LA) using a long sheath (SL0, St Jude Medical, Minneapolis, MN, USA). Left atrial access was gained through a single transeptal puncture or via a PFO. A single bolus of heparin (50IU/kg) was administered after left atrial access had been achieved. ACT was subsequently measured every 45 minutes and an ACT range of 270 to 330 sec was targeted.

Definition of CFAE during sinus rhythm and CS-paced rhythm

CFAE during sinus rhythm (SR) or CS-paced rhythm (CSp) were defined as fractionated potentials exhibiting ≥4 deflections from the isoelectric line with continuous electrical activity (without an isoelectric line) (8).

Definition of CFAE during atrial fibrillation

See under *"CFAE mapping during AF".*

Study protocol

In all patients, the left atrium underwent high density mapping for CFAE in AF, SR and during CS pacing before any ablation was performed. Maps in each of the rhythms comprised greater than 400 points. If the patient presented in AF, the CFAE map in AF was completed first, after which the patient was electrically cardioverted to SR, in order to acquire the SR and CS-paced maps. If the patient presented in SR, the SR and CS-paced maps were acquired first. AF was then induced using burst pacing from CS. We waited for 10 minutes to exclude self-terminating AF prior to performing the CFAE map in AF. 3 patients with longstanding persistent AF could not be electrically cardioverted to SR and were excluded from the study. Following completion of the mapping protocol, patients underwent stepwise AF ablation (9).

Electroanatomical Mapping of CFAE—Following creation of a detailed LA geometry (NavX, Version 8, St Jude Medical, Minneapolis, MN, USA), electrograms were acquired at high density using a 20-polar AFocus II HD catheter (St Jude Medical) registered at multiple left atrial sites. This represented >1200 sites per patient and >400 sites per map. Using the AFocus II HD catheter, each data acquisition provided 19 simultaneous bipolar electrogram (EGM) recordings at the given catheter position. All mapped LA sites were checked manually for accurate annotation.

CFAE mapping during AF—During atrial fibrillation the automatic "CFEmean" detection algorithm of NavX (St Jude Medical) was applied to create the CFAE maps (10, 24). To obtain accurate CFAE mapping during AF, we recorded at each LA site for 8 seconds. CFEmean was calculated by NavX for the whole recording period of 8 seconds for each registered LA site. CFEmean refers to a measure of fractionation derived from the mean interval between electrograms at each site. Continuous CFAE was defined as a CFEmean value of <80ms with a refractory period setting of 40 ms and detection of EGMs exceeding 0.05 mV ("Low-VID") (24, 11).

In order to prevent far-field electrograms from being falsely counted as low voltage or fractionated (5), we reduced the accepted electrogram projection distance to 4mm (to LA geometry); i.e. EGMs with a distance exceeding 4mm from NavX created LA geometry, were not included on the map.

CFAE mapping in sinus rhythm (SR) and coronary sinus paced rhythm (CSp) —In SR a high-density activation map was created of the left atrium comprising >400 points (Figure 1A). In order to assess number and distribution of fractionated EGMs during SR, we visually scrutinized all recorded EGMs and labelled them manually according to the number of deflections from baseline using a linear scale on the NavX system (Figure 1B). LA electrograms with 4 deflections are represented as blue and ≥5 deflections as purple. The borders of areas of fractionation were outlined using the white surface markers.

For CS pacing, the mid coronary sinus was paced at a rate 5–8 beats per minute faster than the intrinsic sinus rate. Attention was paid to exclude ectopic beats and to obtain a

homogenous paced activation map. The pacing rate was limited to slightly faster than the intrinsic rate to minimise any impact of heart rate on fractionation (12). The mid coronary sinus was chosen as it was felt to be a reliable, reproducible site for pacing. It would also give a contrasting left atrial activation pattern to SR (with regard to the direction of the main activation front). The CFAE map was created as for SR. Regions of electrogram fractionation during CS-pacing were outlined using the black surface markers (Figure 1D).

Quantification of CFAE area—The NavX 3D-electroanatomic system allows for measurement of distances and surfaces on the 3D cardiac shell based on electrode size and inter-electrode spacing of introduced catheters ("field-scaling"). The system enables accurate distance and surface measurements on the 3-D LA geometry. To compare quantitatively the overlapping areas of CFAE during AF and SR, AF and CS-pacing and SR and CS-pacing, the surfaces of overlapping CFAE regions between these rhythms were measured for each patient and each rhythm combination. Furthermore, the total LA endocardial surface (including the left atrial appendage and the first 1 cm of the pulmonary veins) on the NavX geometry was measured in each patient. Thus the relation of the CFAE surface to the total left atrial surface could be calculated.

Analysis of mechanism of fractionation during SR and CSp—In order to analyse the prevalence of functional electrogram fractionation, isochronal activation maps were used to create propagation movies. Detailed analysis of LA isochronal maps and propagation maps during SR and CSp was performed to distinguish functional electrogram fractionation (e.g. due to areas of wave-collision) from fractionation due to regional slow conduction or structural remodelling (fixed fractionation during different rhythms).

Correlation of Voltage with degree of fractionation (CFEmean) during AF—For each point taken during CFAE mapping in AF the NavX system calculated a mean voltage measurement corresponding to the mean electrogram voltage during the 8 second period and also a CFE_{mean}. Data were downloaded for each patient allowing correlation of $CFEA_{mean}$ with mean bipolar voltage at each LA site.

Statistical analysis

Continuous data are presented as mean ± standard deviation. Groups were then compared. In absence of normal distribution of data, the non-parametric Mann-Whitney U Test was used. Wilcoxon signed-rank tests were used for paired data. Categorical data were analysed with Fishers exact test. Pearson correlation coefficient was used to calculate correlation between electrogram fractionation and bipolar voltage. Exponential line fitting was chosen based on the equation: $y = ax^b$. The median with the first and third quartiles (Q1, Q3) are reported for skewed data with asymmetric distribution (figure 5C).

A P-value <0.05 was considered statistically significant. SPSS (IBM, NY) was used for statistical analysis.

Results

3 patients with PsAF failed to cardiovert electrically and were excluded from the study. Therefore 18 patients completed the study protocol. Patient characteristics are outlined in Table 1. At the time of the procedure 13 patients presented in AF.

Left atrial high density mapping

A total of 21,096 electrograms were analyzed in 18 patients during AF, SR and CS pacing. This represented 479+/−208 sites per map and >1150 sites per patient. The number of points

per map was comparable between the different rhythms (AF 463 +/−136; SR 470+/−186 and CS-pacing 471+/−243 sites). The mean mapping point density per cm2 was 4.31+/−1.0 points/cm2 on the SR map, 4.61+/−0.96 points/cm2 on the CS-paced map, and 4,79+/−1.53 points/cm2 on the CFEmean maps during AF.

After manual/visual assessment of each electrogram, electrograms with <4 deflections were considered as non-fractionated and were removed from the map. Thereby, only the fractionated electrograms with > 3 deflections remained on the LA geometry. During Sinus rhythm and CS-paced rhythm 8+/−3% and 8+/−2% of all recorded left atrial electrograms were found to be fractionated (>3 deflections), respectively.

Quantitative assessment of CFAE area in AF, SR and CS-pacing

Persistent vs Paroxysmal AF—Quantification of continuous CFAE area during AF demonstrated that in patients with persistent AF (PsAF) CFAE cover a significantly greater percentage of the left atrial surface compared to paroxysmal AF (PAF) patients (27±4% vs 19±9% respectively, p=0.01, Figure 2 & Table 2 upper section). In contrast, in SR and during CSp there was no significant difference in the relative extent of fractionated LA sites between paroxysmal and persistent AF cases (SR: 19±6% vs. 21±7%, respectively, p=0.55; CSp 21±12% vs. 14±5%, respectively, p=0.16).

However, when analyzing the absolute surface areas of fractionated sites during sinus rhythm (SR) or CS-pacing (CSp), we observed significantly higher amount of fractionation (>3deflections from zero line) in patients with persistent AF (PsAF) vs. paroxysmal AF (PAF). The absolute surface area containing fractionated EGMs in SR was found to be 30.8+/−8.1 cm2 vs. 20.0+/−5.4cm2 (in PsAF vs. PAF patients, p=0.019). The absolute surface area with fractionated EGMs in CSp was 29.1+/−16.6 cm2 vs. 14.7+/−4.6 cm2 (PsAF vs. PAF patients, p=0.047). Finally, the absolute surface area with continuous CFAE (CFEmean<80ms) during AF was measured at 37.6+/−5.8 vs. 17.7+/−3.1 (in PsAF vs. PAF patients, p=0.00003).

When these absolute areas of EGM fractionation were put into relation to patient's total left atrial (LA) surface, the differences diminished, because of higher LA size in patients with PsAF, so that the relative surface areas of EGM fractionation did not differ anymore between the 2 groups during SR and CSp.

Comparison of CFAE extent during AF, SR and CSp—The area of the left atrium demonstrating continuous CFAE in PsAF patients was 27±4% during AF, 21±7% in SR and 21±12% during CS pacing (Table 2, upper section). In patients with PsAF, the area of continuous fractionation (during AF) was significantly larger than fractionation in SR (p=0.048). There was no significant difference in fractionation in PsAF vs. CS-paced rhythm (27±4% during AF vs. 21±12% during CS pacing, p=0.12). PAF patients demonstrated consistent levels of fractionation in all three rhythms (AF 19±9%; SR 19±6%, CS pacing 14±5%; AF vs. SR, p=0.9 and AF vs. CS-pacing, p=0.06).

Comparison of CFAE distribution in AF, SR and CSp

In both PAF and PsAF patients little anatomical correlation (overlap) exists between the distribution of CFAE sites in different rhythms (Tables 2 middle and lower section, Figure 3). We calculated the region of concomitant fractionation during 2 rhythms (i.e. (a) AF and SR, (b) AF and CSp and (c) SR and CSp) as the percentage of total fractionation during AF for (a) and (b) and as percentage of fractionated sites during CSp for (c).

In PAF patients, the following amounts of overlap of CFAE sites were found: (a) AF and SR 16+/−4% (b) AF and CS-pacing 6+/−3% (c) SR and CS-pacing 31+/−13%. Similarly, in patients with PsAF, overlap was (a) AF and SR 15+/−5%; (b) AF and CS-pacing 18+/−7%; (c) SR and CS-pacing 29+/−8%. The overall anatomical correlation in all patients was (a) AF and SR 15+/−4%, (b) AF and CSp 12+/−8% and SR and CSp 30+/−10%. Figure 3 highlights the poor anatomical correlation of CFAE seen in AF and SR or CS pacing in a patient with PsAF. When examined as a fraction of the entire left atrial surface, less than 5% of the total surface area demonstrated fractionation during both AF and SR (in both PsAF and PAF patients, Table 2 middle section). A negligible amount of the left atrium appeared fractionated in all three rhythms (Figure 3D).

Mechanism of CFAE in SR and CS-pacing

In patients with PsAF, 27+/−9% of fractionated LA sites were fractionated both during sinus rhythm and CS-pacing (similar result in PAF patients and the total study population: 31+/−13% and 30+/−10%, respectively). Analysis of activation maps and propagation animations performed during SR and CS pacing, revealed local wave collision that could explain 71% of fractionated electrograms (Figure 4A&C, supplemental material: propagation movies of sinus and CS-paced rhythms). Another putative mechanism identified was ‘dyssynchronous’ activation around a zone of slow conduction representing 24% of fractionation in these cases (Figure 4B and D). 5% of remaining fractionated sites could not be explained by these mechanisms.

Correlation of fractionation with electrogram bipolar voltage in AF

Correlation of the fractionation interval (as a surrogate for the degree of fractionation during AF) with the mean electrogram bipolar voltage in AF, demonstrated an inverse CFEmean–voltage relationship during atrial fibrillation (Pearson correlation coefficient $r = -0.32$ for the whole study population, $p<0.0001$, range: −0.28 to −0.50 for individual patients, Figure 5D). More fractionated LA sites showed higher bipolar voltages during AF. Although this correlation is low when including all mapped LA sites (fig. 5D), the inverse voltage relationship is more enhanced when comparing regions surrounding the CFAE sites with LA sites that locate within CFAE sites (figure 5B).

A quantitative analysis of the mean EGM voltage from CFAE maps of patients with PsAF was undertaken. Therefore, a total of > 2000 EGM were exported from CFAE maps. The bipolar voltage at LA sites with continuous CFAE (CFEmean < 80 ms) is significantly higher than at sites without evidence of CFAE (CFE-mean > 120ms) (median: 0.53mV (Q1, Q3: 0.33–0.83) vs. 0.30 mV (Q1, Q3: 0.18–0.515, respectively, $p<0.00001$; mean values: 0.65+/−0.48 mV vs 0.52+/−0.52 mV respectively, $p<0.0001$; Figure 5C).

Left atrial overall mean bipolar voltage during AF in persistent vs. Paroxysmal AF patients

Analysis of the overall global LA voltage during AF in persistent vs. paroxysmal AF patients revealed lower voltages in persistent AF patients than in paroxysmal AF patients: The global overall mean LA voltage in persist. vs. paroxysmal AF patients is 0.6+/−0.59mV vs. 1.12+/−1.32mV ($p<0.01$). In contrast, we did not find any regions of reduced bipolar voltage during sinus or CSp rhythms (all mapped sites had a voltage >1.0 mV in SR or CSp). This shows the functional alterations in EGM voltage during AF. Continuous CFAE sites in AF did not display low voltage in SR. Moreover, continuous CFAE sites displayed higher voltages than non-CFAE sites during AF. It is interesting that the global LA voltage during AF is a discriminating factor between AF type (persistent vs. paroxysmal).

However, these voltage differences are present during AF only. Both the regions of reduced voltage occurring around CFAE sites and regions of higher voltage within the CFAE sites show normal voltage values (>1.0mV) during sinus rhythm or CS-paced rhythm.

Discussion

The key finding of the current study is that both the quantity and the distribution of CFAE within the atria of patients with atrial fibrillation are highly rhythm dependent. EGM fractionation depends on both direction of activation (SR vs. CSp) and rate of activation (SR vs. AF) (12). Less than 5% of the left atrium demonstrates fractionation in both AF and SR. Furthermore, in sinus rhythm the majority of CFAE arise passively as a result of 'wavelet collision' at sites that display normal bipolar voltages, suggesting absence of myocardial fibrosis/scar. These sites of wave-collision are unlikely to represent effective targets for ablation.

High density mapping of CFAE

Targeting of CFAE is a frequently used strategy during the catheter ablation of persistent AF (1;13–19). However the exact role of CFAE in the pathogenesis of AF remains unclear. Indeed, not all CFAE ablation impacts upon AF tachycardia cycle length implying that not all CFAE play a role in AF perpetuation (7;9). Hence unnecessary ablation is being performed. Greater comprehension of CFAE is required to improve the specificity of ablation techniques.

High density mapping has increased the quality of CFAE mapping allowing >400 points to be acquired per map and hence strengthening its use both clinically and as a research tool. Miyamoto et al have previously assessed CFAE volume in SR and AF but with only 76±22 points per AF map, using an 8mm tip catheter with lower mapping resolution (20). Using these methods, they found CFAE in AF at 42% of the left atrial surface. The discrepancy in percentage of the surface area demonstrating fractionation between that study and the current report (CFAE at 28% of the LA surface in PsAF) reflects the high density mapping used in the current study (reducing the interpolation resulting from using fewer points) and the cut-off value for CFE_{mean} used to ≤80msec (measuring more continuously fractionated signals compared to CFE_{mean} ≤120msec that includes sites of intermittent EGM fractionation during AF). Furthermore, the exclusion of points with an electrogram projection distance of greater than 4mm to the left atrial geometry prevents registration of points with poor contact and/or farfield signals as fractionation previously recognised as a common cause of 'CFAE' (5;21). Therefore, the current study demonstrates increased density of mapping and identifies sites of greater fractionation. Finally, accuracy of each map was improved by manual assessment of all electrograms. EGMs with evidence of low catheter contact or artefact were excluded from map and analysis.

Extent of CFAE in PsAF vs. PAF

High density mapping confirms increased fractionation in the atria of patients with PsAF (28±4%) than those with PAF (16±4%). This observation has been described previously (11;22). Interestingly, pulmonary vein isolation during the ablation of PsAF results in an altered distribution and a significant reduction in left atrial pre-ablation fractionation without termination (23), suggesting in turn that much of the pre-ablation fractionation in the left atrium may play a passive role. Furthermore, ablation of those continuous CFAE that persisted both before and after PVI has been associated with a higher rate of AF termination (23). Hence, persistence of CFAE in changing left atrial conditions may be a marker of CFAE resulting from fixed or pathological tissue changes (scar). Therefore, the current

study aimed to identify LA sites that remain persistently fractionated in different rhythms (AF, SR and CSp).

The spatial distribution of CFAE sites in AF, SR and CS-pacing

Figure 3C highlights areas of fractionation identified in a single atrium during SR (white markers) and CS pacing (black markers). Note the different patterns of fractionation, but that in both rhythms fractionation tends to localise close to the pulmonary vein ostia and also the inter-atrial septum. This is in direct contrast to CFAE maps taken in AF where fractionation is identified in the body of the atrium (red markers in figures 2 and 3A&B). Quantification of areas of overlapping fractionation during AF, SR and CSp identified only a very small amount of anatomical overlap between fractionated LA sites in SR and CFAE regions in AF. In total <5% of the LA surface demonstrated fractionation in both rhythms. Moreover, LA sites with persistent fractionation in all 3 rhythms are rare, implying that most of the fractionation in AF arises in areas that appear entirely normal in sinus rhythm - in terms of bipolar voltage and degree of fractionation. This does not exclude an active role for these CFAE in propagating AF, but does argue that the fractionation may be a function of the complex atrial electrical activity during AF rather than an underlying atrial disease process that is associated with localized atrial scar.

We also describe that distribution of fractionation differs between SR and CS pacing (Figure 3C). Indeed there is only a 30% correlation between the two rhythms (again representing <5% of the total LA surface area). This implies that despite both being regular stable rhythms with comparable cycle lengths, it is the direction of activation within the atrium that defines location and volume of fractionation, rather than characteristics of the local left atriala myocardium.

Mechanism of CFAE in SR and CSp

Using epicardial recordings in patients without a history of AF, Konings et al. showed previously that fractionation of unipolar EGM during induced AF occurs at sites of a) conduction slowing/block, b) pivot points of wavelets, c) asynchronous activation and d) at sites of wave collision (3). In addition, Rostock et al. revealed that bipolar electrogram fractionation depends on the local activation rate/cycle length. The shorter the cycle length, the more fractionated the electrograms (so called “fibrillatory conduction”) (12). Lellouche et al. found a link between some of the fractionated LA sites in SR and parasympathetic (vagal) responses during RF-ablation at those sites (8). Currently, ablation of CFAE sites (in AF) constitutes part of the routine ablation strategy for PsAF. However, even when ablating continuous CFAE during AF, an impact on AF cycle length/termination is observed in only 50% of ablated LA sites (6).

High density mapping during SR and CS pacing provides detailed activation maps that in turn give insight into the mechanism of fractionation within atrial myocardium. Figure 4A (during SR) and 4C (during CSp) represent isochronal activation maps demonstrating clear evidence of wave collision at an area of fractionation (71% of fractionated sites in SR/CSp). The site of fractionation depends on the vector of the left atrial activation in SR and CS-pacing, that determines the region of wave-collision. In Figure 4A (during SR) the wave of depolarisation wraps around the left atrium and the wavelets collide under the left inferior pulmonary vein. In Figure 4C (during CSp) a long region of wavelet collision is identified at the roof of LA (between the right and left superior pulmonary veins). This long line of wave collision at LA roof, results in a long area of fractionated EGMs during CSp rhythm (black markers), that is not present during sinus rhythm.

An alternative mechanism is seen in Figures 4B and 4D. 'Dyssynchronous' activation is noted around a zone of slow conduction that corresponds to a fractionated area (24% of fractionated sites in SR/CSp). In contrast to the passive nature of wave collisions, anisotropic conduction and dyssynchronous activation may reflect electrophysiological properties of the local myocardium crucial to AF maintenance.

Not all fractionation identified during high density mapping can be explained by these two mechanisms, however they can be repeatedly identified giving rise to a large proportion of fractionation during SR and CS-pacing. Moreover, an unexpectedly low percentage of the LA was fractionated in both AF and SR. This suggests that a) there is minimal fixed fractionation b) there is probably a high proportion of passively formed CFAE in AF and c) that fractionation identified in SR is unlikely to represent a good target for ablation. Finally, it is noteworthy that common sites of overlap between AF and SR were located at the PV antrum and LA septum. Furthermore, areas of overlap in all three rhythms were rare, but when present, they localized to PV ostia or septum. Such regions merit further examination and could represent critical targets in AF ablation.

Analysis of CFAE areas in AF with regard to electrogram voltages both in AF and SR

During SR, bipolar voltage maps of the left atrium display normal voltages (>1.0 mV) within the atrial body in all patients (data not shown). Regions of reduced bipolar voltage during SR were only found within the pulmonary veins.

Analysis of the bipolar voltage during the 8-second recording period for each recorded EGM in AF, revealed a mean voltage of 0.596 mV for the total number of EGM recorded during AF (in all patients). Interestingly, areas of functional lower voltage (<0.5mV) were found during AF within the left atrial body (Figure 5B) and appeared to surround regions of continuous CFAE. When compared to CFAE maps during AF in the same chamber (Figure 5A), continuous CFAE regions (CFEmean <80ms) correlate with areas of higher voltage in AF. This image of lower voltage sites surrounding continuous CFAE sites was consistently found in all patients during AF. Furthermore, quantitative analysis of mean bipolar voltage during AF at continuous CFAE sites (CFEmean<80ms) vs non-CFAE sites (CFEmean>120ms) showed a significantly higher voltage at CFAE than at non-CFAE sites with an inverse correlation between mean fractionation interval (CFEmean) as a surrogate of 'degree of fractionation' in AF and mean voltage in AF (Figures 5C&D). This result confirms that low voltage in AF is functional and that areas of continuous fractionation during AF do not correspond to low voltage and diseased atrial tissue. Moreover, continuous CFAE sites display higher voltage during AF than surrounding (non-fractionated) LA sites. This finding may be related to the fibrillatory wave dynamics/wave-collisions during AF that result in globally reduced bipolar voltages during AF vs. SR. Moreover, less fractionated LA sites that surround continuous CFAE sites display even lower voltage during AF.

Left atrial overall mean bipolar voltage during AF in persistent vs. Paroxysmal AF patients

Analysis of the overall global LA voltage during AF in persistent vs. paroxysmal AF patients revealed lower voltages in persistent AF patients than in paroxysmal AF patients (0.6+/−0.59mV vs. 1.12+/−1.32mV, $p<0.01$). It is interesting that the global LA voltage during AF is a discriminating factor between AF type (persistent vs. paroxysmal). However, these voltage differences are present during AF only. Both the regions of reduced voltage occurring around CFAE sites and regions of higher voltage within the CFAE sites show normal (>1.0mV) voltage values during sinus rhythm or CS-paced rhythm.

CFAE Mapping using NavX Algorithm (CFEmean)

CFEmean is a widely used algorithm that is integrated into the NavX system. The method has been used and evaluated by other authors with regard to the temporal stability of CFAE sites in AF (24). Aizer *et al.* (25) demonstrated that a standardized and validated algorithm for the identification of fractionation, using an FI <120 ms, refractory window of 49 ms, and signal width of 10 ms could achieve a sensitivity of 0.75 and specificity of 0.80. Tsai WC et al. (26) re-evaluated the automatic CFAE detection algorithm of the NavX with regard to Nademanee's criteria: In their analysis, the automatic CFAE algorithm exhibited the highest combined sensitivity and specificity with a CFEmean (fractionation interval (FI)) of <60 ms for the sites within areas of low voltage in SR (<0.5mV) and a CFEmean < 70 ms for the sites with a voltage value > 0.5mV.

Based on our experience with visual assessment of CFAE sites and higher probability of AF cycle length prolongation when ablating continuous CFAE sites (displaying continuous activity during AF) (8), we defined LA sites with CFEmean values < 80ms as best corresponding to continuous CFAE sites with our reported refractory settings (refractory period: 41ms).

If the refractory settings are changed from 41 to 49ms and the CFEmean is considered as up to 120ms range, the extent of CFAE in AF will be larger (because also CFEmean interval value between 80 and 120ms are added to the map). However, the CFAE map still looks similar with its original outer limits being little extended. When comparing these surfaces with fractionated sites during SR or CSp, the important discrepancy in the spatial distribution between the rhythms still remains.

The settings we used to detect continuous CFAE sites (CFEmean up to 80ms, refractory window of 41ms) highlight the core of CFAE sites with higher fractionated EGMs during AF, with an attenuation of surrounding intermittent fractionated sites (CFEmean 80–120ms).

Nademanee et al. first described ablation of CFAE sites in AF as a electro-physiological substrate based ablation of AF (1). They described regions <0.15mV as low voltage during AF. However this was not the criterion that they used to guide ablation (1). Using high density mapping with up to 900 mapped LA sites per rhythm (figure 1, 5), we observed EGMs of reduced mean voltage during AF (<0.5mV) that surround higher voltage EGMs at sites with continuous CFAE. However, both CFAE sites and sites of reduced voltage in AF (surrounding CFAE sites) showed normal voltage in SR and CSp (>1.0 mV), proving the functional nature of the dispersion in mean bipolar voltage during AF. Future studies, focusing on activation pattern and local activity rates during AF may give explanation to these observations.

Limitations

The shape, voltage and degree of fractionation of bipolar EGM recordings depend on the orientation of the recording bipole with regard to the regional/local wave propagation. By using the 20-polar double-loop catheter, we could reduce the probability that certain LA sites where only mapped in one bipole orientation only (because similar LA regions were mapped through different catheter positions).

The absence of simultaneous entire LA chamber mapping during AF, does not allow determination of the instantaneous LA fractionation. Simultaneous recording of the AF over the entire LA (and RA) would be the best method to get deeper understanding of the fibrillatory mechanism and to characterize the instantaneous local cycle lengths and evaluate extent of fractionated LA sites during AF. However, even the serial acquisition of CFAE maps using point-by-point mapping technique with the ablation catheter have shown a

certain temporal consistency in the CFAE maps up to 78% (24). We applied high density mapping using a circumferential 20-electrode catheter with a diameter of 20mm that enables simultaneous EGM recording over the catheter surface area (5 to 7cm2). Using this method, the high density map could be generated in <10 minutes during AF. The mapping time did not exceed 10 minutes in case of SR and CSp-rhythms.

Owing to the post processing required to identify and map out areas of fractionation in the three rhythms, correlation of highly fractionated areas was not possible in real-time. Hence ablation could not be targeted at the <5% of the LA total surface area that demonstrated fractionation in both AF and SR. Such a strategy, examining for cycle length prolongation may represent a goal for future work.

Conclusions

This paper describes high density mapping of the left atrium performed during atrial fibrillation (AF), sinus rhythm (SR) and coronary sinus pacing (CSp). We observe that the distribution of fractionation is highly rhythm dependent, and that there is little overlap between areas that are fractionated in each rhythm. Most fractionated EGMs during SR or CS-pacing result from wave-collisions. Therefore, targeting fractionated LA sites during SR (or CSp) does not seem to present a more specific strategy in order to identify pro-arrhythmogenic LA sites. The work provides evidence that CFAE areas that are presently targeted for AF ablation, represent areas of atrial myocardium with normal voltage (>1.0mV) and EGM morphology in sinus rhythm, excluding structural scar as underlying substrate. Thus, a substantial part of CFAE sites in AF may correspond to regions of wave-collision and represent passive CFAE that may play little role in the perpetuation of atrial fibrillation. Further studies are warranted to identify those CFAE sites that actively perpetuate atrial fibrillation.

Supplementary Material

Refer to Web version on PubMed Central for supplementary material.

Acknowledgments

Funding Sources: This work has been supported by grants from the Leducq Foundation and the French Society of Cardiology. AJ obtained fellowship grant from Hopitaux Universitaires de Genève (Switzerland) and StJMed.

References

1. Nademanee K, McKenzie J, Kosar E, Schwab M, Sunsaneewitayakul B, Vasavakul T, Khunnawat C, Ngarmukos T. A new approach for catheter ablation of atrial fibrillation: mapping of the electrophysiologic substrate. J Am Coll Cardiol. 2004; 43:2044–2053. [PubMed: 15172410]
2. Hunter RJ, Berriman TJ, Diab I, Baker V, Finlay M, Richmond L, Duncan E, Kamdar R, Thomas G, Abrams D, Dhinoja M, Sporton S, Earley MJ, Schilling RJ. Long-term efficacy of catheter ablation for atrial fibrillation: impact of additional targeting of fractionated electrograms. Heart. 2010; 96:1372–1378. [PubMed: 20483892]
3. Konings KT, Kirchhof CJ, Smeets JR, Wellens HJ, Penn OC, Allessie MA. High-density mapping of electrically induced atrial fibrillation in humans. Circulation. 1994; 89:1665–1680. [PubMed: 8149534]
4. Jais P, Haissaguerre M, Shah DC, Chouairi S, Clementy J. Regional disparities of endocardial atrial activation in paroxysmal atrial fibrillation. Pacing Clin Electrophysiol. 1996; 19:1998–2003. [PubMed: 8945085]
5. Narayan SM, Wright M, Derval N, Jadidi A, Forclaz A, Nault I, Miyazaki S, Sacher F, Bordachar P, Clementy J, Jais P, Haissaguerre M, Hocini M. Classifying fractionated electrograms in human

atrial fibrillation using monophasic action potentials and activation mapping: Evidence for localized drivers, rate acceleration, and nonlocal signal etiologies. Heart Rhythm. 2011; 8:244–253. [PubMed: 20955820]

6. Takahashi Y, O'Neill MD, Hocini M, Dubois R, Matsuo S, Knecht S, Mahapatra S, Lim KT, Jais P, Jonsson A, Sacher F, Sanders P, Rostock T, Bordachar P, Clementy J, Klein GJ, Haissaguerre M. Characterization of electrograms associated with termination of chronic atrial fibrillation by catheter ablation. J Am Coll Cardiol. 2008; 51:1003–1010. [PubMed: 18325439]
7. Hunter RJ, Diab I, Thomas G, Duncan E, Abrams D, Dhinoja M, Sporton S, Earley MJ, Schilling RJ. Validation of a classification system to grade fractionation in atrial fibrillation and correlation with automated detection systems. Europace. 2009; 11:1587–1596. [PubMed: 19897499]
8. Lellouche N, Buch E, Celigoj A, SiEGerman C, Cesario D, De DC, Mahajan A, Boyle NG, Wiener I, Garfinkel A, Shivkumar K. Functional characterization of atrial electrograms in sinus rhythm delineates sites of parasympathetic innervation in patients with paroxysmal atrial fibrillation. J Am Coll Cardiol. 2007; 50:1324–1331. [PubMed: 17903630]
9. O'Neill MD, Wright M, Knecht S, Jais P, Hocini M, Takahashi Y, Jonsson A, Sacher F, Matsuo S, Lim KT, Arantes L, Derval N, Lellouche N, Nault I, Bordachar P, Clementy J, Haissaguerre M. Long-term follow-up of persistent atrial fibrillation ablation using termination as a procedural endpoint. Eur Heart J. 2009; 30:1105–1112. [PubMed: 19270341]
10. Verma A, Novak P, Macle L, Whaley B, Beardsall M, Wulffhart Z, Khaykin Y. A prospective, multicenter evaluation of ablating complex fractionated electrograms (CFEs) during atrial fibrillation (AF) identified by an automated mapping algorithm: acute effects on AF and efficacy as an adjuvant strategy. Heart Rhythm. 2008; 5:198–205. [PubMed: 18242539]
11. Solheim E, Off MK, Hoff PI, Schuster P, Ohm OJ, Chen J. Characteristics and distribution of complex fractionated atrial electrograms in patients with paroxysmal and persistent atrial fibrillation. J Interv Card Electrophysiol. 2010; 28:87–93. [PubMed: 20386973]
12. Rostock T, Rotter M, Sanders P, Takahashi Y, Jais P, Hocini M, Hsu LF, Sacher F, Clementy J, Haissaguerre M. High-density activation mapping of fractionated electrograms in the atria of patients with paroxysmal atrial fibrillation. Heart Rhythm. 2006; 3:27–34. [PubMed: 16399048]
13. Verma A, Sanders P, Macle L, Champagne J, Nair GM, Calkins H, Wilber DJ. Selective CFAE Targeting for Atrial Fibrillation Study (SELECT AF): Clinical Rationale, Design, and Implementation. J Cardiovasc Electrophysiol. 2011; 22:541–547. [PubMed: 21087332]
14. Kong MH, Piccini JP, Bahnson TD. Efficacy of adjunctive ablation of complex fractionated atrial electrograms and pulmonary vein isolation for the treatment of atrial fibrillation: a meta-analysis of randomized controlled trials. Europace. 2011; 13:193–204. [PubMed: 21037322]
15. Singh JP, Ptaszek LM, Verma A. Elusive atrial substrate: complex fractionated atrial electrograms and beyond. Heart Rhythm. 2010; 7:1886–1890. [PubMed: 20817015]
16. Hunter RJ, Berriman TJ, Diab I, Baker V, Finlay M, Richmond L, Duncan E, Kamdar R, Thomas G, Abrams D, Dhinoja M, Sporton S, Earley MJ, Schilling RJ. Long-term efficacy of catheter ablation for atrial fibrillation: impact of additional targeting of fractionated electrograms. Heart. 2010; 96:1372–1378. [PubMed: 20483892]
17. Lin YJ, Tai CT, Chang SL, Lo LW, Tuan TC, Wongcharoen W, Udyavar AR, Hu YF, Chang CJ, Tsai WC, Kao T, Higa S, Chen SA. Efficacy of additional ablation of complex fractionated atrial electrograms for catheter ablation of nonparoxysmal atrial fibrillation. J Cardiovasc Electrophysiol. 2009; 20:607–615. [PubMed: 19642225]
18. Oral H, Chugh A, Yoshida K, Sarrazin JF, Kuhne M, Crawford T, Chalfoun N, Wells D, Boonyapisit W, Veerareddy S, Billakanty S, Wong WS, Good E, Jongnarangsin K, Pelosi F Jr, Bogun F, Morady F. A randomized assessment of the incremental role of ablation of complex fractionated atrial electrograms after antral pulmonary vein isolation for long-lasting persistent atrial fibrillation. J Am Coll Cardiol. 2009; 53:782–789. [PubMed: 19245970]
19. Oral H, Chugh A, Good E, Wimmer A, Dey S, Gadeela N, Sankaran S, Crawford T, Sarrazin JF, Kuhne M, Chalfoun N, Wells D, Frederick M, Fortino J, Benloucif-Moore S, Jongnarangsin K, Pelosi F Jr, Bogun F, Morady F. Radiofrequency catheter ablation of chronic atrial fibrillation guided by complex electrograms. Circulation. 2007; 115:2606–2612. [PubMed: 17502567]
20. Miyamoto K, Tsuchiya T, Nagamoto Y, Yamaguchi T, Narita S, Ando S, Hayashida K, Tanioka Y, Takahashi N. Characterization of bipolar electrograms during sinus rhythm for complex

fractionated atrial electrograms recorded in patients with paroxysmal and persistent atrial fibrillation. Europace. 2010; 12:494–501. [PubMed: 20167615]

21. Narayan SM, Franz MR. Quantifying fractionation and rate in human atrial fibrillation using monophasic action potentials: implications for substrate mapping. Europace. 2007; 9(Suppl 6):vi89–vi95. [PubMed: 17959699]
22. Lo LW, Lin YJ, Tsao HM, Chang SL, Hu YF, Tsai WC, Tuan DC, Chang CJ, Lee PC, Tai CT, Tang WH, Suenari K, Huang SY, Higa S, Chen SA. Characteristics of complex fractionated electrograms in nonpulmonary vein ectopy initiating atrial fibrillation/atrial tachycardia. J Cardiovasc Electrophysiol. 2009; 20:1305–1312. [PubMed: 19804543]
23. Lin YJ, Tai CT, Kao T, Chang SL, Lo LW, Tuan TC, Udyavar AR, Wongcharoen W, Hu YF, Tso HW, Tsai WC, Chang CJ, Ueng KC, Higa S, Chen SA. Spatiotemporal organization of the left atrial substrate after circumferential pulmonary vein isolation of atrial fibrillation. Circ Arrhythm Electrophysiol. 2009; 2:233–241. [PubMed: 19808473]
24. Roux JF, Gojraty S, Bala R, Liu CF, Hutchinson MD, Dixit S, Callans DJ, Marchlinski F, Gerstenfeld EP. Complex fractionated electrogram distribution and temporal stability in patients undergoing atrial fibrillation ablation. J Cardiovasc Electrophysiol. 2008; 19:815–820. [PubMed: 18373601]
25. Aizer A, Holmes DS, Garlitski AC, Bernstein NE, Smyth-Melsky JM, Ferrick AM, Chinitz LA. Standardization and validation of an automated algorithm to identify fractionation as a guide for atrial fibrillation ablation. Heart Rhythm. 2008; 5:1134–1141. [PubMed: 18675224]
26. Tsai WC, Lin YJ, Tsao HM, Chang SL, Lo LW, Hu YF, Chang CJ, Tang WH, Tuan TC, Udyavar AR, Wang JH, Chen SA. The Optimal Automatic Algorithm for the Mapping of Complex Fractionated Atrial Electrograms in Patients With Atrial Fibrillation. J Cardiovasc Electrophysiol. 2009 Jul 28.

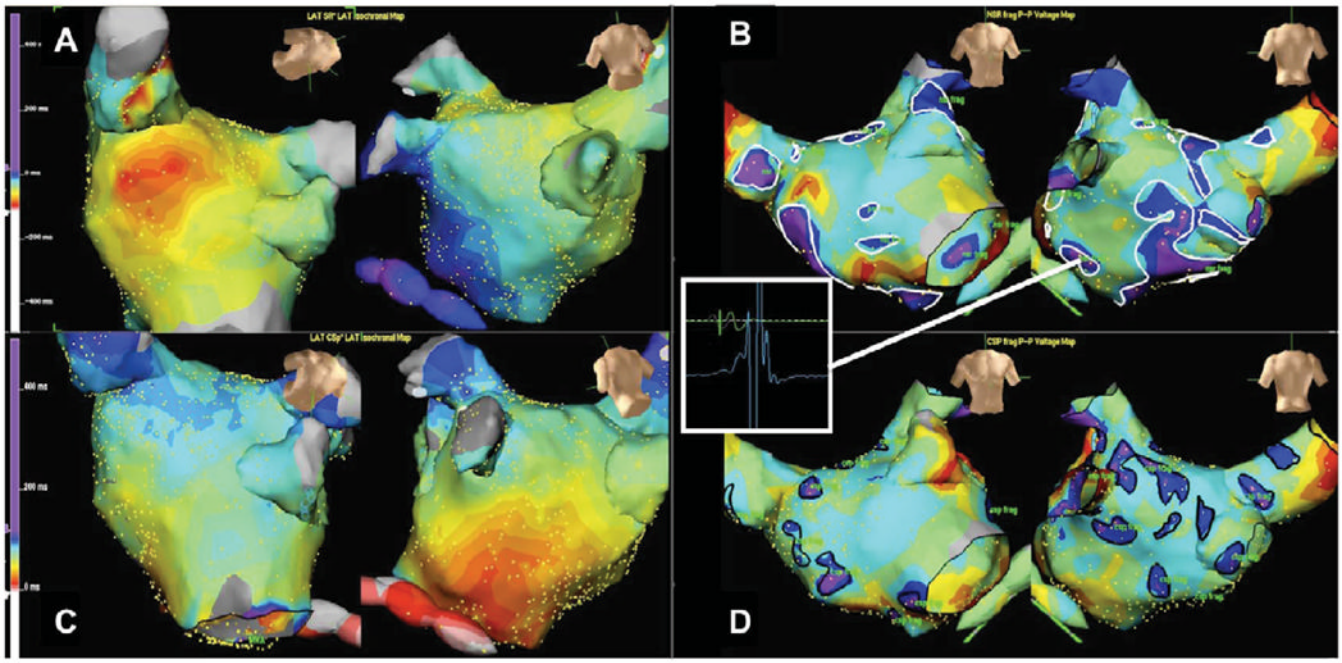

Figure 1.

Activation and CFAE maps in Sinus Rhythm and during CS pacing in the same left atrium. A&C demonstrate the high density of points (>700 points/map in this patient) taken and the activation map thus created in SR and during CS pacing respectively. Figures B&D demonstrate CFAE maps in SR and CS pacing respectively. The colour scales in maps (B) and (D) reflect the number of deflections of the electrogram from baseline. CFAE are in dark blue and purple (>4 and >5 deflections respectively). Regions of CFEA thus identified are ringed in markers (SR = white, CSp = black). Note the different distribution of fractionation during SR and CS pacing at similar heart rates.

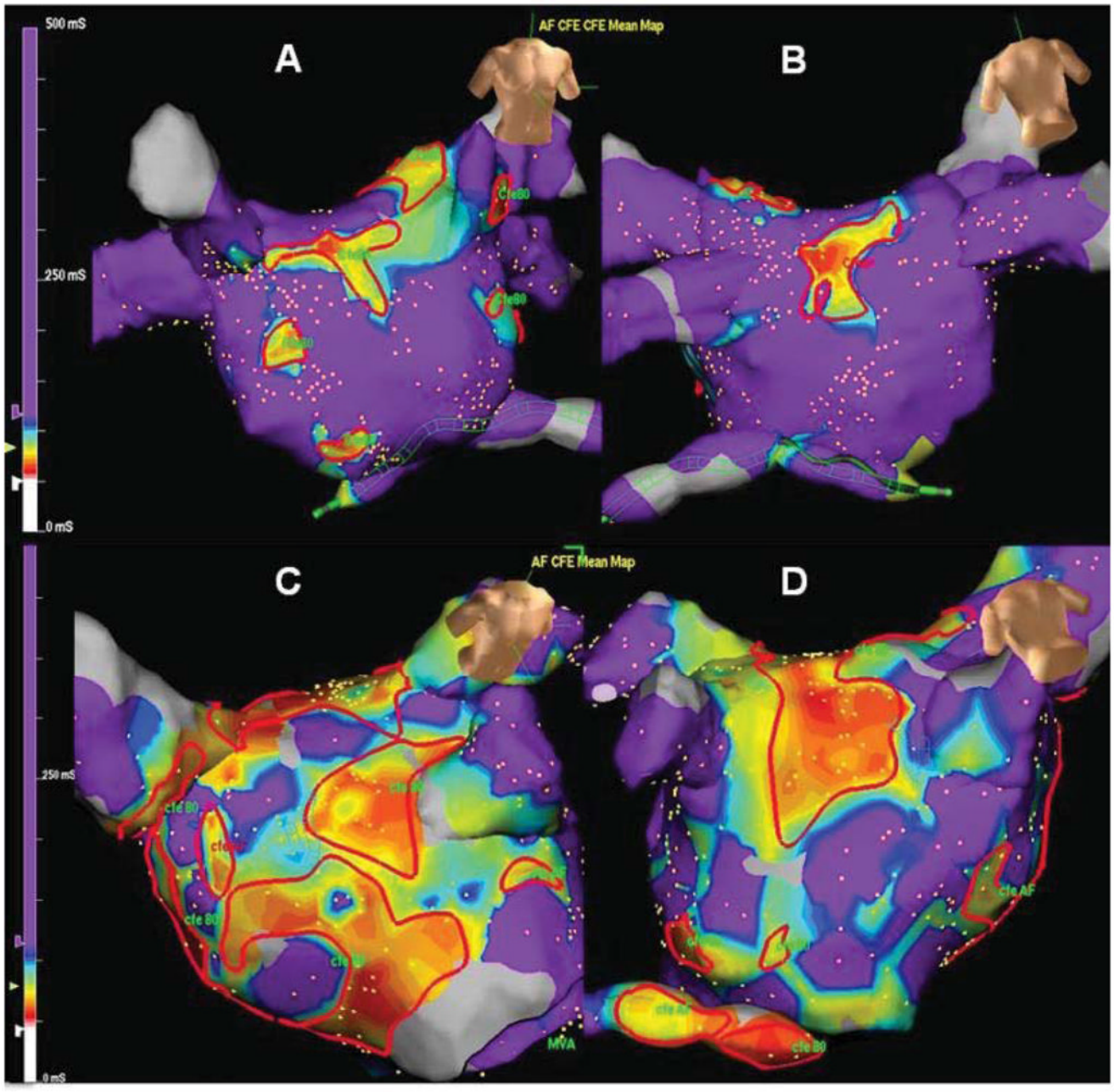

Figure 2.

Distribution of CFEA during atrial fibrillation. High density CFAE map recorded in AF in a patient with PAF (A&B) and PsAF (C&D – same patient as figure 1). Significantly more CFAE were identified in PsAF patients compared to PAF (p=0.02). Continuous CFAE sites (CFEmean <80ms) are outlined in red.

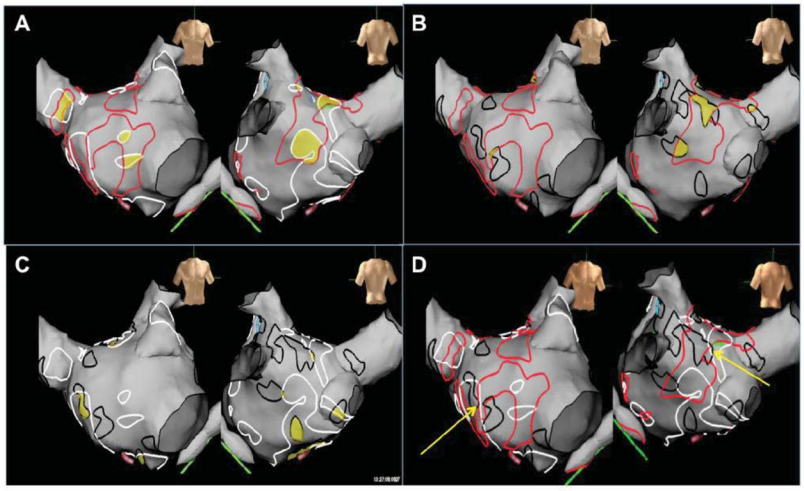

Figure 3.

Correlation of CFAE distribution during atrial fibrillation, sinus rhythm and CS pacing. High density CFAE map recorded in the same patient as Figure 1. (A) Comparison of regions of CFAE in AF and SR. (B) Comparison of regions of CFAE in AF and CS paced rhythm. (C) Comparison of CFAE distribution in SR and CS paced rhythm. (D) Comparison of all three rhythms. Continuous CFAE sites in AF were marked in red, electrogram fractionation in SR and during CS-pacing in white and black respectively. Overlapping CFAE sites between different rhythms are highlighted as yellow areas. Mean overlap of CFAE areas in [AF + SR] and [AF and CS-p] were only 15+/−5% and 18+/−7% of the total CFAE area in AF, respectively. Only 27+/−9% of LA sites show fractionation during both SR and Cs-pacing (yellow areas in C). Less than 5% of the total LA surface area was fractionated in both AF and SR. A negligible amount of the left atrium appeared fractionated in all three rhythms. In the current case areas appear to border each other but not overlap (areas highlighted by yellow arrows (D)).

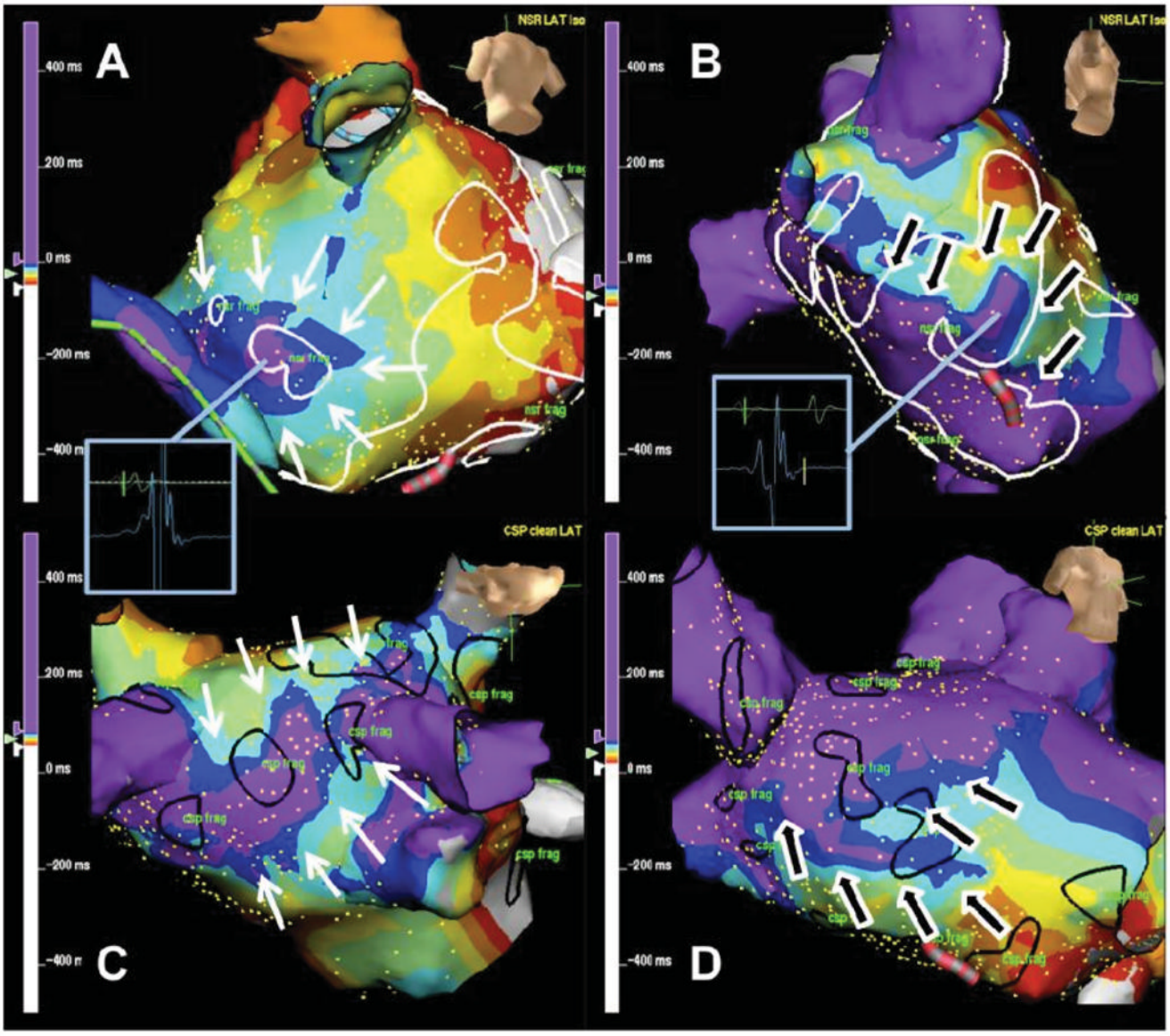

Figure 4.

Isochrone activation map of the left atrium during SR and CS pacing characterising mechanisms of fractionation. Figures A&C demonstrate examples of ‘wavelet collision’ during SR and CS pacing respectively. White arrows highlight the direction of waves of depolarisation that collide at areas of fractionation. In Figures B&D depolarisation is seen to wrap around a zone of slow conduction (black arrows) resulting in ‘dyssynchronous’ activation of that region corresponding to an area of fractionation. Regions of fractionation in SR are outlined with white markers (upper panels), CS paced in black (lower panels).

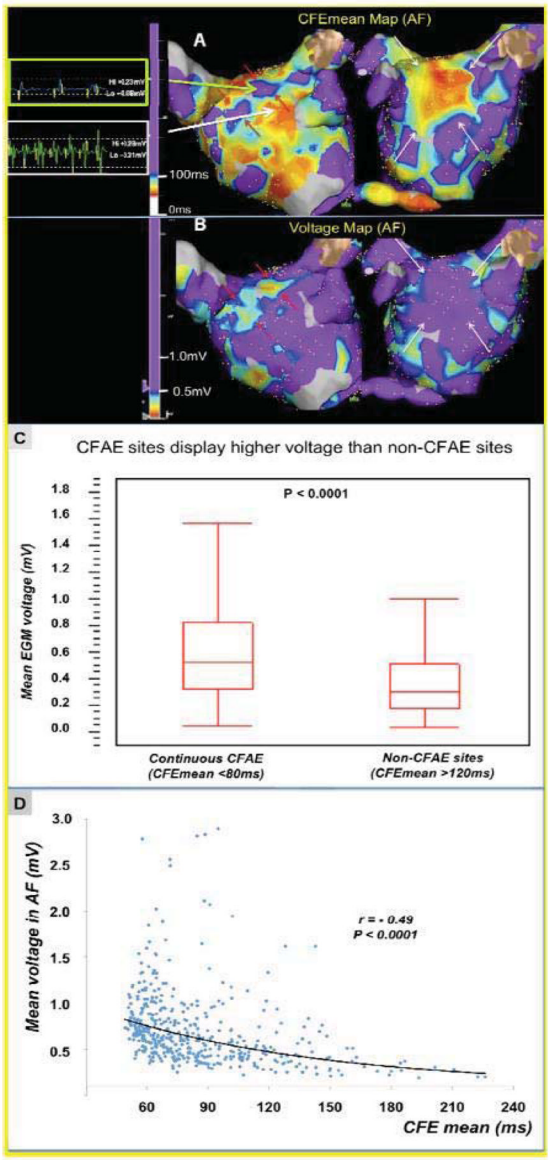

Figure 5.

Correlation of degree of electrogram fractionation with mean bipolar voltage during AF. CFAE (A) and Voltage (B) maps of the same left atrium taken during AF. Typically areas without fractionation correspond to sites of reduced voltage (<0.5mV) surrounding CFAE sites in Panel A and B (red arrows; green arrow shows a representative low voltage EGM surrounding anterior CFAE site). Conversely, the large area of CFAE on the anterior wall demonstrated higher voltage electrograms (>0.5mV; large white arrow shows representative EGM). (C) Quantitative analysis of > 2800 EGs (CFAE maps in AF, recording time 8 seconds) in the PsAF patients. Continuous CFAE sites (CFEmean <80ms) display higher bipolar voltage during AF than non-CFAE sites (CFEmean>120ms) (median: 0.53mV (IQR: 0.33–0.83) vs. 0.30 mV (IQR: 0.18–0.515, respectively, p<0.00001). (D) Example of inverse correlation between CFEmean interval (surrogate of fractionation in AF) and mean EG voltage in a patient with persistent AF (r= −0.49, p<0.0001).

Table 1

Patient characteristics

	Total population (18 patients)	Paroxysmal AF (PAF) (9 patients)	Persistent AF (PsAF) (9 patients)	P Value (PAF vs. PsAF)
Age	59.0+/−7	58.6+/−6	59+/−8	P = 0.89
Male (%)	15 (83)	7 (77)	8 (89)	P = 1.0
Structural Heart Disease (%)	6 (33)	2 (22)	4 (44)	P = 0.62
Hypertension (%)	5 (55)	2 (22)	3 (33)	P = 1.0
Failed AADs	2.1+/0.7	2.0+/0.7	2.2+/−0.7	P = 0.59
LA diameter (mm)	44.1+/−7.7	38.9+/−2.1	49.4+/−7.8	P = 0.005
LVEF (%)	59.5+/−5.2	60.7+/−4.5	58.2+/−5.8	P = 0.39

Table 2

Quantification analysis of CFAE sites during AF, SR and CS-pacing.

	PAROXYSMAL AF	PERSISTENT AF	p-Value
CFAE as percentage of total LA surface area			
AF	19±9%	27±4% *	0.01
SR	19±6%	21±7% *	0.55
CSp	14±5%	21±12%	0.16
Overlap between CFAE in different rhythms as percentage of total LA surface			
AF and SR	3+/−1%	4+/−2%	0.09
AF and CSp	1+/−1%	5+/−2%	<0.001
SR and CSp	4+/−2%	6+/−2%	0.16
CFAE regions in AF also fractionated in SR and CSp			
SR	16+/−4%	15+/−5%%	0.93
CSp	6+/−3%	18/−7%	<0.001

* In patients with PsAF, there is a significantly higher extent of continuous CFAE sites in AF versus the extent of fractionated LA surface in sinus rhythm (CFAE at 27+/−4% of the total LA surface vs. fractionation at 21+/−7% during sinus rhythm, p=0.048).